

Geophysical Research Letters[®]

RESEARCH LETTER

10.1029/2021GL097647

Key Points:

- Event synchronization analysis provides a novel understanding on the teleconnection between oceans and precipitation in Northeast Brazil (NEB)
- The dominant role of the tropical North Atlantic on precipitation is captured by episodic phase lockings particularly in recent decades
- We identify the indirect El Niño–Southern Oscillation–Atlantic interactions having significant influence on and reinforcement for NEB droughts

Supporting Information:

Supporting Information may be found in the online version of this article.

Correspondence to:

Y. Zou,
yzou@phy.ecnu.edu.cn

Citation:

Mao, Y., Zou, Y., Alves, L. M., Macau, E. E. N., Taschetto, A. S., Santoso, A., & Kurths, J. (2022). Phase coherence between surrounding oceans enhances precipitation shortages in Northeast Brazil. *Geophysical Research Letters*, 49, e2021GL097647. <https://doi.org/10.1029/2021GL097647>





Received 4 JAN 2022

Accepted 16 APR 2022

Author Contributions:

Conceptualization: L. M. Alves, E. E. N. Macau, A. S. Taschetto, A. Santoso
Formal analysis: Y. Mao, Y. Zou
Investigation: Y. Mao, Y. Zou, L. M. Alves, A. S. Taschetto, A. Santoso
Methodology: E. E. N. Macau, J. Kurths
Writing – original draft: Y. Zou, L. M. Alves, E. E. N. Macau, A. S. Taschetto, A. Santoso, J. Kurths
Writing – review & editing: Y. Zou, L. M. Alves, E. E. N. Macau, A. S. Taschetto, A. Santoso, J. Kurths

Phase Coherence Between Surrounding Oceans Enhances Precipitation Shortages in Northeast Brazil

Y. Mao¹, Y. Zou¹ , L. M. Alves² , E. E. N. Macau^{2,3}, A. S. Taschetto⁴ , A. Santoso^{4,5} , and J. Kurths^{6,7}

¹School of Physics and Electronic Science, East China Normal University, Shanghai, China, ²Instituto Nacional de Pesquisas Espaciais, São Paulo, Brazil, ³Federal University of São Paulo, São Paulo, Brazil, ⁴Climate Change Research Centre and ARC Centre of Excellence for Climate Extremes, University of New South Wales, Sydney, NSW, Australia, ⁵Centre for Southern Hemisphere Oceans Research, CSIRO Oceans and Atmosphere, Hobart, TAS, Australia, ⁶Potsdam Institute for Climate Impact Research, Potsdam, Germany, ⁷Department of Physics, Humboldt University Berlin, Berlin, Germany

Abstract Understanding the direct and indirect impact of the Pacific and Atlantic Oceans on precipitation in the region of Northeast Brazil (NEB) is crucial for monitoring unprecedented drought events. We propose nonlinear methods of phase coherence and generalized event synchronization analysis to understand the underlying mechanism. In particular, the relationships between sea surface temperature (SST) variability and the standard precipitation index are interpreted as direct interactions, while the relationships between surrounding oceans are interpreted as indirect effects on the precipitation. Our results reveal a dominant role of tropical North Atlantic for precipitation deficit and droughts, particularly in recent decades. Meanwhile, the indirect Pacific–North Atlantic phase synchronizations have significant influence on and reinforcement of the droughts in NEB. Furthermore, we find that the instantaneous angular frequencies of precipitation and SST are drastically changed after very strong El Niño and La Niña events, therefore resulting in a higher probability of phase coherence.

Plain Language Summary Atmospheric teleconnections are coherent climate responses across the globe and commonly identified by large distance correlations, which have been largely included in climate analysis. Still, the nonlinear features of teleconnections to many places across the globe, including Northeast Brazil (NEB), have not been fully understood. Here, we propose a nonlinear framework of combining phase coherence with event synchronization analysis to further understand the teleconnections between the surrounding oceans and precipitation in NEB, which has been affected significantly by extreme droughts in the recent decade. We find that the North Atlantic Ocean plays a dominant role in affecting NEB rainfall variability. We also show that this influence has become more persistent in recent years compared to the impact from the tropical Pacific. At the same time, the teleconnection between Pacific and North Atlantic has also become more frequent in recent years, which suggests that these tropical ocean basin interactions reinforced the NEB droughts in recent decades.

1. Introduction

Since 2012 the semiarid region of Northeast Brazil (NEB) has been experiencing a continuous dry condition, that is, some years of extremely dry condition and other years of extreme rain (Marengo et al., 2017). In the recent decade, the drought in the Northeast Brazil shows one of the most significant impacts on population and regional economy in its history. Using soil and vegetation indices, the period of 2011–2016 has been identified as the 5 years most severe and prolonged drought since satellite era (Brito et al., 2018). Poor rainfall during the rainy season affected reservoir water availability with severe consequences for urban supply and economic losses in agriculture and livestock (Alvalá et al., 2019). Therefore, the Northeast Brazil has been considered as one of the world's most vulnerable regions to extreme climate events of severe droughts and floods (Marengo et al., 2019).

The atmospheric teleconnections to NEB have been extensively studied for decades (Cai et al., 2020; Hastenrath & Heller, 1977; Moura & Shukla, 1981; Rodrigues & McPhaden, 2014; Uvo et al., 1998). Both observational and climate model results point out that oceanic and atmospheric conditions from the tropical Atlantic and Pacific basins influence precipitation patterns over NEB on different timescales (Rodrigues et al., 2011). For example, on seasonal timescales, the rainy seasons in South America have been significantly determined by the Intertropical

Convergence Zone (ITCZ) (Hastenrath & Heller, 1977) which is directly influenced by the tropical Atlantic sea surface temperature (SST) anomalies. During abnormal warmer periods of North Atlantic (NA) SST, the ITCZ is anomalously northward positioned which in consequence causes a shortage of rainfall in NEB. On the other hand, the presence of positive South Atlantic (SA) SST anomalies favors the southward displacement of the ITCZ, which in extreme cases causes floods in NEB. Meanwhile, El Niño-Southern Oscillation (ENSO) (Timmermann et al., 2018) can also impact NEB precipitation via direct or indirect means (Rodrigues et al., 2011). Usually, ENSO influences precipitation anomalies over the NEB directly via changes in the zonally oriented Walker circulation subsidence (Cai et al., 2020; Kane, 1997). In addition, the ENSO also strongly affects the NEB indirectly via changes in the tropical North Atlantic SST (Rodrigues et al., 2011; Taschetto et al., 2016; Uvo et al., 1998; Wang, 2004). The North Atlantic (NA) variability has a strong dependence on the ENSO-related atmospheric anomalies through a midlatitude “atmospheric bridge,” the so-called Pacific-North American teleconnection, which further influences the positions of ITCZ, especially during the rainy seasons. These direct and indirect interactions between oceans may explain the findings that only part of drought events in the NEB have been attributed to ENSO, while other events are due to the tropical Atlantic SST variability (Kayano & Andreoli, 2006; Marengo et al., 2017).

Due to the nonlinearity of the climate system, modern time series analysis tools originated from complexity science provide novel perspectives on assessing teleconnections on various timescales. For example, complex network representation of the climate system has been successfully applied to characterize distinctive roles of El Niño and La Niña events (Meng et al., 2020; Wiedermann et al., 2016), providing early warnings of El Niño events (Ludescher et al., 2014, 2021), and extreme rainfall events (Boers et al., 2019). On the other hand, time series network approaches provide interdisciplinary platforms for nonlinear time series analysis (Zou et al., 2018). From the viewpoint of methodology, we propose in this work to combine two previously separated methods of phase coherence analysis (Maraun & Kurths, 2005; Singh et al., 2020) and event synchronization analysis (Boers et al., 2013; Malik et al., 2012; Quián Quiroga et al., 2002) to assess the teleconnections in the NEB region during the recent period of extensive droughts. Here we show that the dominant role of tropical NA SST for precipitation deficit and droughts in NEB is successfully captured by our nonlinear method, which is not straightforward to be obtained using either of these two methods individually. Meanwhile, our method readily reveals that the indirect ENSO-NA phase synchronizations have significant influence on and reinforcement of the droughts. We point out that the instantaneous angular frequency changes of SST variabilities are due to different modulation capacity of very strong El Niño and La Niña events, therefore resulting in a higher probability of phase coherence.

2. Materials and Methods

2.1. Data and Standard Precipitation Index

We use data of the Climate Prediction Center gauge based analysis of global unified daily precipitation for the period from 1981 to 2020 (Cai et al., 2020; Chen et al., 2008), and the NOAA V2 high-resolution blended analysis of daily SST for the same period (Huang et al., 2021). We choose four regions of interest as shown in Figure 1a: NEB region that has been the center of drought in recent decades; Niño3 is a region of intense ENSO activity and strong teleconnections to NEB (Cai et al., 2020; Hastenrath, 1990); NA and SA regions, both similar areas used in previous studies (Kayano & Andreoli, 2006; Kayano et al., 2018). Meanwhile, we check the consistency of our results by choosing Niño4 in the Central Pacific and extended SA region (Rodrigues & McPhaden, 2014). The corresponding discussions are included in the Supporting Information S1 (SI, Section 1). For each domain we calculate the spatial average of the variable of interest and calculate the daily anomalies relative to a base period of 1981–2010. Rainy seasons are defined from January to April and dry seasons are from May to August.

The Standard Precipitation Index (SPI) is a widely used measure to characterize drought on a range of timescales, which has been used for drought monitoring and forecasting (McKee et al., 1993). In Figures 1b and 1c, we show the 3-month scale SPI values. In the recent decade (starting from 2012), drought events appear more frequently in both the rainy and dry season (Figures 1b and 1c), when the SPI is continuously negative and reaches an intensity of -1.0 or less. In addition, no significant difference is found for the drought events in either rainy (35.9% of all drought events), dry seasons (34.4% of all drought events), or the rest of the year (32.8% of all events happened from September to December) (Figure 1d), which is confirmed by SPI values at all scales from 3 to 24 months. We emphasize that this SPI figure provides only partially a description on the climate conditions of short-term

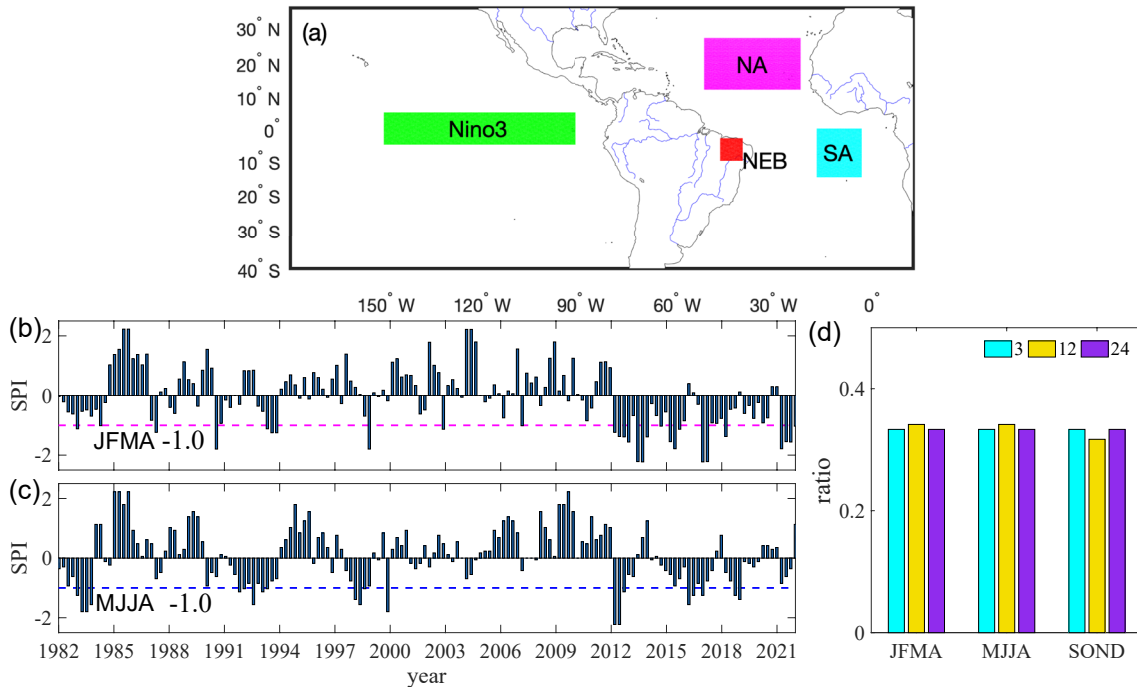


Figure 1. (a) Geographic domains. Northeast Brazil (NEB) region: (45°W–38°W, 10°S–3°S); tropical North Atlantic (NA): (50°W–20°W, 12°N–27°N); tropical South Atlantic (SA): (15°W–0°E, 15°S–0°N), and Niño3: (150°W–90°W, 5°S–5°N). Further regions of Niño4 and extended SA are considered in the Supporting Information S1 (SI). (b–d) The 3-month scale Standard Precipitation Index (SPI) for NEB. (b) Rainy seasons and (c) dry seasons. The horizontal dashed line is the threshold to define drought events. (d) The occurrence ratios of drought events in different seasons (SPI at scales of 3, 12 and 24 months). SOND: from September to December.

soil moisture and crop stress during the growing season, while the limits of SPI interpretations are acknowledged (Wu et al., 2007).

For the phase coherence analysis below, we apply the third order Butterworth filtering to low-pass filter the SPI and SST time series in the spectral domain, that is, frequencies higher than 0.7 cycles per year are damped, which therefore help us in disclosing phase relations of inter-annual oscillations (Figure S1 in Supporting Information S1).

2.2. Phase Coherence Analysis

The phase coherence analysis was originally introduced to understand interactions between two weakly coupled chaotic oscillators (Rosenblum et al., 1996), which has found wide applications in climate sciences, that is, identifying phase coherence between ENSO and the Indian monsoon (Maraun & Kurths, 2005; Singh et al., 2020), and that between the South American monsoon system and Rossby waves (Gelbrecht et al., 2018).

First, the phase components of the SST anomaly time series $x(t)$ of the Niño3 and NA are respectively denoted as $\Phi_i(t)$ and $\Phi_j(t)$, which are extracted via Hilbert transformation (Section 2.2 in Supporting Information S1). The next step is to calculate the phase difference between two signals which is denoted as $\phi_{m,n}(t) = m\Phi_i(t) - n\Phi_j(t)$, where the subscripts m, n are integers and i, j represent different geographical locations. Phase locked windows are captured when the phase difference $\phi_{m,n}(t)$ is bounded, namely, $|\phi_{m,n}| < C$, where C is a constant. The selection criteria for phase locked epochs are such that consecutive points of periods are at least longer than 1 year in the same plateau in the phase difference plot (Section 2.3 in Supporting Information S1).

We use surrogate techniques to test the significance of the phase-locked plateaus against the null hypothesis of mutually independent processes with corresponding spectral properties as the original SST (Maraun & Kurths, 2005). Taking the Niño3-NA interaction as an example, we generate 1,000 surrogates for the Niño3 SST by phase randomization in the spectral domain. Then, we perform the same phase coherence computations between each of the realizations and the original NA SST and choose the 950 maxima (out of 1,000 realizations)

as the 95% significance level. Only those phase locked epochs passing this 95% significance level will be discussed below. Furthermore, the degree of phase coherence are captured by both coherence order parameter R and the coherence index ρ (Section 2.4 in Supporting Information S1).

2.3. Event Synchronization Between Phase Epochs and Extreme Drought Events

Starting from the phase difference series $A = \phi_{m,n}(t)$, we denote a phase locked plateau by the arrival time position and the corresponding plateau length, that is, an interval for the phase locked plateau $[t_i^A, t_i^A + \Delta T_i]$. The total number of plateaus is denoted as N_A . In addition, based on the SPI values (Figure 1), we identify a drought event if SPI is smaller than -1.0 , timings of which are denoted as $t_0^B, t_1^B, \dots, t_j^B$ with annotations of N_B dry events. The phase locked plateau length ΔT_i has not been fully considered in the traditional event synchronization analysis, which instead regards the entire plateau as one single event (Singh et al., 2020). The explicit inclusion of ΔT_i helps to quantitatively characterize the synchronization levels between different locations.

The generalized event synchronization analysis for all plateaus and extreme dry events are performed as follows (sketched in Figure S8 of Supporting Information S1):

1. *co-occurrence rate (CR)* computes the co-occurrence rate of dry events that are in phase locked epochs, that is,

$$CR = \frac{\sum_j^{N_B} \# \{t_j^B \cap \Delta T_i^A, \text{ for all } i\}}{N_B}. \quad (1)$$

This quantity is large if more dry events fall into phase locked plateaus.

2. *precursor rate of phase locked plateaus*: Following with event coincidence analysis (Donges et al., 2016), we compute a generalized precursor rate to quantify the causal effects of different temporal phase locked plateaus on the dry events. Since each phase locked plateau shows different coupling delays, we shift the dry event series by time delay ΔT_i by τ_i , which is varied from 1 to 4 months for each phase locked epoch (Wu et al., 2020). The precursor rate of phase plateau ΔT_i is then calculated by the average number of dry events in this time shifted phase epoch, that is,

$$r_{p,i} = \frac{1}{\Delta T_i} \# \{(t_j^B - \tau_i) \in [t_i^A, t_i^A + \Delta T_i]\}, \text{ for all } t_j^B. \quad (2)$$

The overall precursor rate of all plateaus is then summarized as $r_p = \sum_i^{N_A} r_{p,i}$. Large value of r_p means that there are more dry events coincident with the phase locked windows, which therefore suggests a stronger causal effect by the phase coherent interactions.

2.4. Frequency Modulations of Extreme Events

First, we denote the instantaneous frequency series as $d\Phi_i(t)/dt$ which is obtained by the time derivative of the corresponding phase variable $\Phi_i(t)$ of SST and SPI (Section 2.2 in Supporting Information S1). To reveal the instantaneous frequency changes due to strong events, we separate the frequency series of each component into five time windows depending on the presence of El Niño and La Niña events. More specifically, according to the definitions of El Niño and La Niña events (Trenberth, 1997), we divide the whole time axis (1 January 1981–31st December 2020) into five non-overlapping windows of (a) strong El Niño (≥ 1.5 , sElNiño), (b) weak El Niño ($0.5 \sim 1.5$, wElNiño), (c) normal periods without events ($-0.5 \sim 0.5$, NoEvents), (d) weak La Niña ($-1.3 \sim -0.5$, wLaNiña), and (e) strong La Niña (≤ -1.3 , sLaNiña). Note that the thresholds for La Niña events are better chosen for Niño4 SST series. In consequence, we have five distribution functions of the instantaneous frequency for each window.

Next, we show the instantaneous frequency changes in different windows, while taking the normal periods without events (NoEvents) as the reference for comparison. Taking the Niño3 frequency series as an example, we compare the distribution functions of the frequencies in the two time windows of (i) strong El Niño events (sElNiño) and (iii) the NoEvents by using a quantile-quantile (Q-Q) scatter plot (Singh et al., 2020). A Q-Q plot is created by plotting quantiles of sElNiño against NoEvents quantiles. If both sets of quantiles come from the same

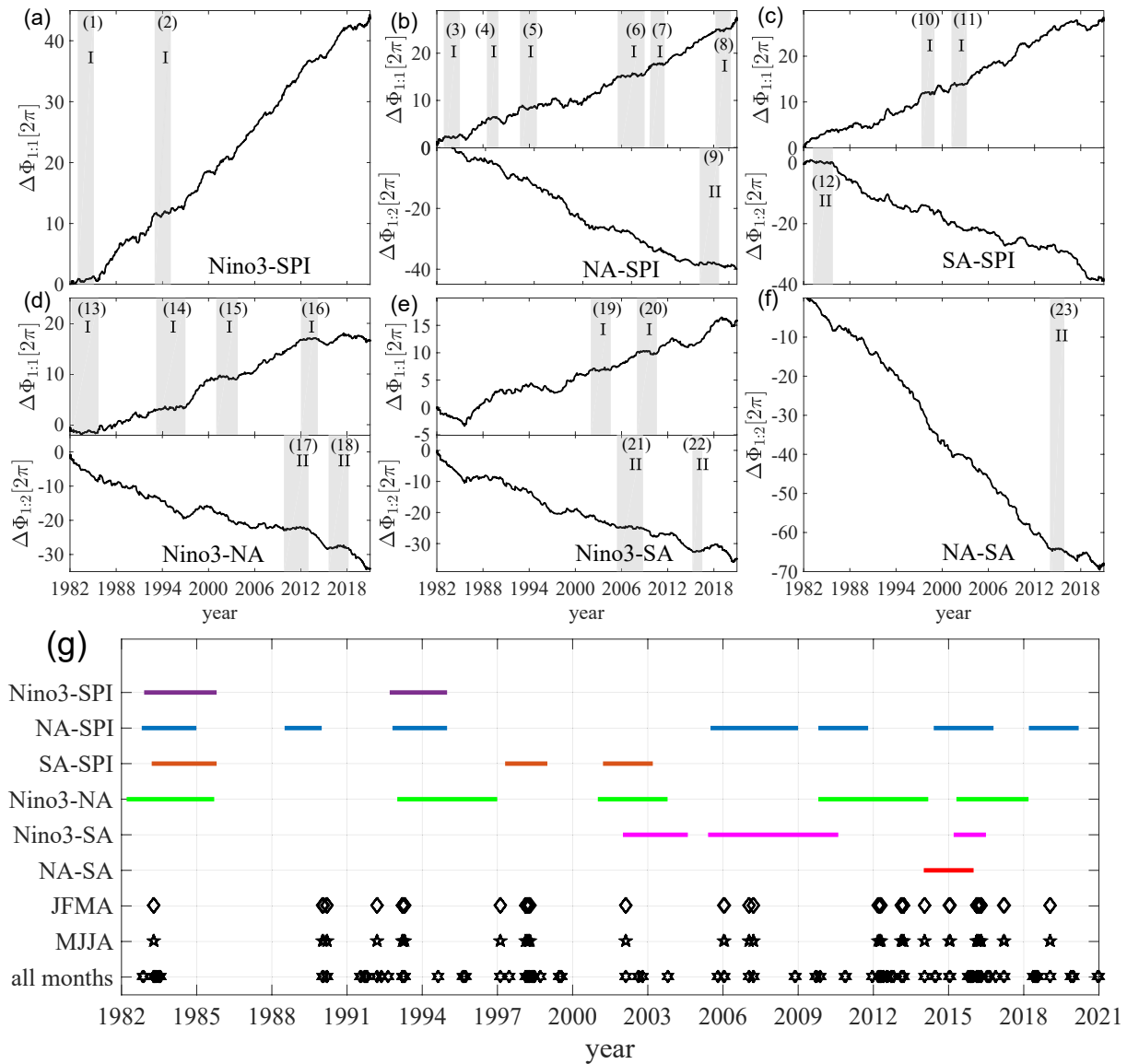


Figure 2. (a–c) Phase difference between the oceans and Standard Precipitation Index (SPI). (a) Niño3–SPI (1:1), (b) NA–SPI (upper: 1:1 and bottom: 1:2), and (c) South Atlantic (SA)–SPI (upper: 1:1 and bottom: 1:2). Time windows of phase locked plateaus have been highlighted by Gy bars and 1:1 phase locking is denoted by the Roman number I, and respectively, II is for 1:2 locked windows. (d–f) Phase difference between oceans. (d) Niño3–NA (upper: 1:1 and bottom: 1:2), (e) Niño3–SA (upper: 1:1 and bottom: 1:2), and (f) NA–SA (1:2). (g) Summary of phase locked plateaus (top six rows) and extreme dry events (bottom three rows). Drought events have been separated into three categories: (i) rainy seasons, (ii) dry seasons and (iii) all months.

distribution, we expect the points are aligned forming a Line of Identity in the scatter plot, while the deviations reflect the difference in the two sets of quantiles.

3. Results

3.1. Phase Locked Epochs Between the Ocean and Precipitation

We report all pairwise phase difference series in Figures 2a–2f showing episodic phase locked epochs. For the phase correlations between the surrounding oceans and the SPI (Figures 2a–2c), we observe 12 phase locked plateaus (each is longer than 1 year), showing different scenarios for different ocean regions. The detailed information of each plateau as denoted by Arabic numbers (including the start and end points, p -value) is summarized in Supporting Information S1 (Table S1). There are seven epochs in the NA–SPI interrelation (Figure 2b). Note

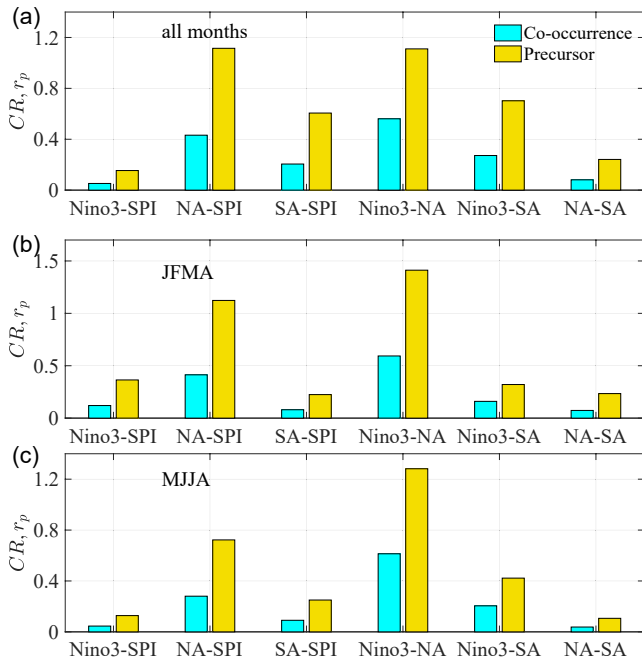


Figure 3. Co-occurrence rates (CR) and precursor rates (r_p) between phase locked plateaus and drought events. (a) All months, (b) rainy seasons, and (c) dry seasons. The indirect Niño3–NA interaction is significantly stronger than the direct NA–Standard Precipitation Index (SPI) interaction.

that phase locking appears more frequently after 2006, which suggest that the NA plays an increasingly dominant role in influencing precipitation patterns in NEB. In contrast, we find there are only two locked epochs of Niño3–SPI and three in SA–SPI, showing less appearance. Figures 2a and 2c further suggests much weaker direct roles of Niño3 and SA on the precipitation. The weak interaction from the Pacific is also confirmed when using the Niño4 index which captures SST variability in the Central Pacific (Figure S6a in Supporting Information S1).

From the viewpoint of direct interactions, the phase coherence analysis reveals that the tropical NA plays a dominant role in influencing the precipitation in the NEB. This direct interaction is explained by the northward position of ITCZ during the warming period of NA, which causes rainfall shortage in the NEB.

3.2. Phase Locked Epochs Between the Oceans

We interpret the phase coherence between different oceans as indirect indicators for the precipitation in the NEB. Interestingly, Figures 2d–2f show that there are more phase locked plateaus in the Niño3–NA relationship. In particular, these epochs of phase locking extend for longer time periods from 2009 till 2018. Meanwhile, the phase coherence of Niño3–SA is weaker in comparison to Niño3–NA, showing phase locked windows in 2004–2008. In addition, Niño4 shows strong phase coherence with the SA (Figure S6c in Supporting Information S1). Although the two chosen North and South Atlantic regions are geographically closer, only one phase locked window is found (Figure 2f), suggesting that the coupling of NA–SA is not significant for understanding of precipitation variations. This result agrees with

the finding that the temperatures in the tropical NA and SA are not always interrelated, as reported by Chang et al. (2006). But the tropical NA warming after an El Niño event can create a significant inter-hemispheric temperature gradient to make the ITCZ position staying longer in the Northern Hemisphere.

The indirect interactions between oceans as an enhancing factors to explain the precipitation patterns. In particular, we argue that the phase locked relationship between the Niño3 and the NA are important for the rainfall shortages, especially for the recent decade. The Walker circulation is displaced eastward under El Niño conditions, which in consequence acts as the main physical driver influencing the ITCZ position. Strong El Niño events modulate the instantaneous frequencies of the NA SST oscillations, which increase the probability of phase coherence, as will be explained below.

3.3. Generalized Event Synchronization Between Phase Epochs and Extreme Drought Events

All phase locked windows are summarized in Figure 2g, which includes drought events for better comparisons. In particular, the event synchronization between the phase locked epochs and extreme drought events are captured by the co-occurrence rates (CR) and precursor rate (r_p) (Figure 3). Besides the strong NA–SPI interactions, we additionally find that there is a significant large frequency of the precursor rate r_p of the Niño3–NA phase locking epochs on the dry events than any others. This conclusion holds for all cases of time spans (a) all months (January to December), (b) wet rainy seasons (JFMA), and (c) dry seasons (MJJA). The drought events outside the rainy seasons could happen because of the increased winds or evaporation (Rodrigues et al., 2011). In contrast, there is no significant coincidence for Niño4–NA phase lockings with drought events (Figure S9 in Supporting Information S1). Instead, we find that the phase locking of Niño4–SA acts as another indirect interaction on drought events in the dry seasons (Figure S9c in Supporting Information S1). Based on this finding, we conclude that the teleconnection of ENSO–Atlantic plays as an enforcement factor on the precipitation in the NEB.

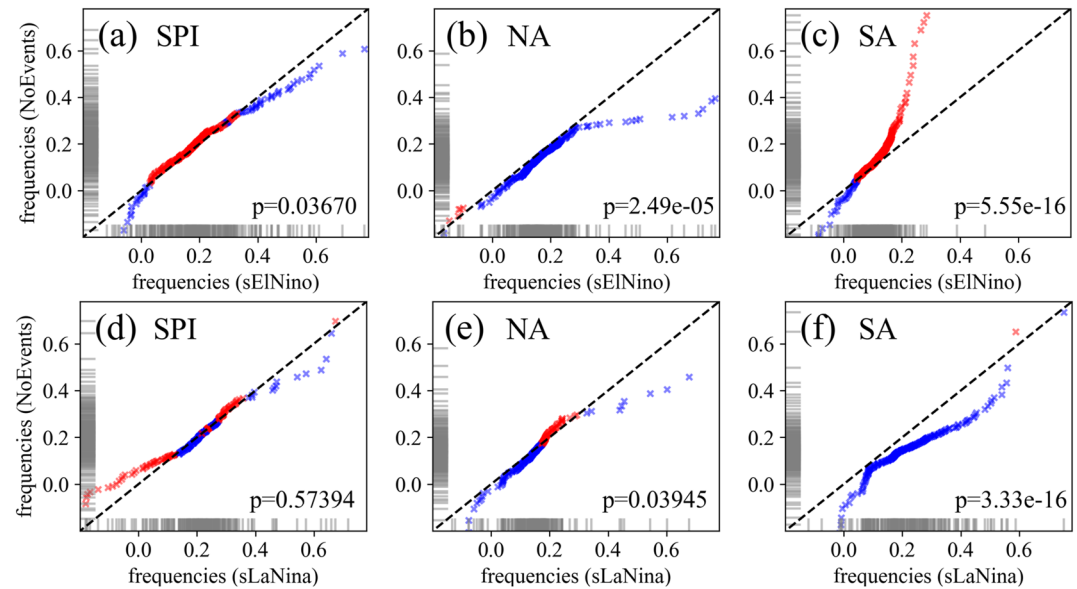


Figure 4. Quantile-Quantile scatter plots comparing the probability distributions of instantaneous frequency for two time windows of (i) strong events (El Niño (a–c) and La Niña (d–f)) and (ii) normal periods without events (NoEvents). (a, d) Standard Precipitation Index (SPI), (b, e) North Atlantic, and (c, f) South Atlantic. The points below the Line of Identity are highlighted by blue (respectively, above are red) and the percentage of points below the diagonal: (a) 23%, (b) 98%, (c) 12%, (d) 57%, (e) 72%, and (f) 98.8%. The p -value by the Kolmogorov-Smirnov test is included in the corresponding legend.

3.4. Frequency Modulations by Strong El Niño and La Niña Events

We show that strong El Niño and La Niña events modulate the instantaneous frequencies of the SST and SPI. A Quantile-Quantile scatter plot of the instantaneous frequencies of SPI between two time windows of strong El Niño (sElNiño) and no events (NoEvents) is shown in Figures 4a–4c. In particular, Figure 4a suggests that strong El Niño events decrease the frequency of SPI (77% points are above the Line of Identity). A Kolmogorov-Smirnov test indicates that the distributions of instantaneous frequency between the sElNiño and NoEvents is significantly different from each other, which therefore increase the probability of ENSO-SPI phase coherence.

Similarly, the Kolmogorov-Smirnov tests suggest that North and SA show statistically significant difference in the distributions of two time windows of sElNiño and NoEvents (Figures 4b and 4c). This clear difference is that strong El Niño events increase the angular frequency of the NA oscillations (98% points are below the Line of Identity in Figure 4b). In contrast, there are 88% lower frequencies (or 12% higher frequencies) of the SA oscillations following the time window of sElNiño, suggesting that strong El Niño decreases the SA variability (Figure 4c).

In addition, strong La Niña events do not modulate frequencies of SPI series directly (Figure 4d, $p > 0.1$). Instead, they yield higher instantaneous frequencies for both the NA (72% points below the Line of Identity in Figure 4e) and the SA (98% points below the Line of Identity in Figure 4f).

We further show that weak El Niño yield similar results as for strong events (Figure S10a–S10c in Supporting Information S1), namely, leading to lower frequencies for SPI oscillation ($p < 0.05$) and larger frequencies for NA oscillation ($p < 0.0001$). However, the frequency modulation for the SA is not significant ($p > 0.1$). In addition, weak La Niña events do not significantly modulate the frequencies of SPI, NA, nor SA oscillations (Figure S10d–S10f in Supporting Information S1, $p > 0.05$).

4. Conclusions

The establishment of teleconnections between two distant locations is recognized as one of the important research areas in climate studies. The underlying non-stationary interactions require nonlinear time series analysis tools to provide statistically reliable estimates. Here, we choose one specific example of teleconnections affecting the

precipitation patterns in NEB, which has been affected significantly by extreme drought events in the recent decade. We reveal distinctive roles of direct interactions between oceans and precipitation and indirect interactions between oceans. To this end, we propose a nonlinear framework combining the event synchronization analysis with phase coherence analysis, which disclose the precursor effects of the phase locked plateaus on the precipitation shortages. Our generalized method reveals the effects of phase locked window length directly, which has been underestimated in the traditional event synchronization analysis. As such, we quantitatively characterize the interaction levels between different locations. In particular, the direct interaction from the tropical NA SST plays a dominant role, which is directly due to the northward positions of the ITCZ during the warming periods. In other words, our results confirm that the precipitation in the NEB are more closely determined by the tropical NA SST variability. In contrast, little evidence is found for possible direct effects of the Niño3 on the precipitation. This rather weak relationship between the ENSO and the NEB rainfall is consistent with Kayano and Andreoli (2006).

We find a significant phase locking behavior between Niño3 and the NA, in which Niño3 region may act as an indirect driving force for the climate condition of the NEB due to higher probabilities of warming SST in the NA following warming periods in the Pacific. The enhanced indirect interaction may be attributed to a combination of factors, such as increased ENSO variability in recent decades (Cai et al., 2021). In addition, the capacitor effect mechanism of warming trend of the Atlantic due to global warming and the positive phase of Atlantic Multi-decadal variability could enhance the influence of NA variability on ENSO (Wang et al., 2017). This means warm (cool) NA in boreal spring leads to La Niña (El Niño) in boreal winter (Ham et al., 2013). This contributes to higher probabilities of phase coherence between ENSO and NA. Therefore, we argue that the rainfall shortage in the rainy seasons has been significantly and indirectly enhanced by the Niño3-NA teleconnection. In addition, this indirect interaction has become more frequent, which may serve as an important indicator for the rainfall shortages in the recent decade. On the other hand, phase coherence between the central Pacific and the tropical SA coincides with droughts more frequently in the dry seasons (Figure S9 in Supporting Information S1), which shows novel understanding for the Pacific—South American atmospheric variability. Note that phase coherence analysis discloses the instantaneous frequency modulation relationship between two variables, while not taking into account the amplitude information. In the Supporting Information S1, we show that no significant correlations are found for the amplitudes between any pair of two variables of this study (Figure S5 in Supporting Information S1).

In addition, we find compelling evidence that strong El Niño and La Niña events result in instantaneous frequency modulations of the NA SST variabilities, which therefore enhance the probability of phase coherence between ENSO and Atlantic variability. More specifically, the warming of the Niño3 SST following very strong El Niño events lead to a lower instantaneous frequency of the SPI oscillations (Figure 4a). In contrast, strong El Niño events increase the frequency of the NA SST oscillations (Figure 4b), which however showing a mixed role of either decreasing or increasing the frequencies of the SA oscillations (Figure 4c). Note that the impact of ENSO on the tropical NA is nonlinear (Casselman et al., 2021) and that weak El Niño events are not able to modulate the frequencies of the oceanic SST variability, which is consistent with Taschetto et al. (2016). In contrast, strong La Niña events do not modulate the frequencies of SPI directly (Figure 4d), instead leading to higher frequencies of the tropical Atlantic oscillations (Figures 4e and 4f).

Our results of the episodic phase coherence at interannual time scales between the SST in Pacific, Atlantic and the SPI in the NEB can help improve regional climate models toward better predictions, particularly in the current changing climate in which ENSO variability has been identified as one of key tipping elements in a changing climate. An important recent advance in understanding ENSO is that El Niño events are diverse in terms of the magnitude, duration, and location of SST anomalies, and future changes in any of these aspects (Cai et al., 2020) are expected to influence various processes via inter-basin interactions, thus calling for further nonlinear phase coherence and event synchronization analysis for such scenarios. Finally, other factors such as land-use changes can lead to changes in the hydrological cycle, as demonstrated by several modeling and observational studies, particularly over the Amazon basin (Lejeune et al., 2015; Marengo et al., 2018). How land-use changes may alter climate characteristics and interactions should motivate further research using the methodology as proposed in this work.

Data Availability Statement

The data that support the findings of this study are openly available: (a) the NOAA High-resolution Blended Analysis of Daily SST at <https://psl.noaa.gov/data/gridded/data.noaa.oisst.v2.highres.html>, respectively, (b) the CPC Global Unified Gauge-Based Analysis of Daily Precipitation at <https://psl.noaa.gov/data/gridded/data.cpc.globalprecip.html>.

Acknowledgments

Parts of this work have been financially supported by the National Natural Science Foundation of China (Grant Nos. 11872182, 11835003, 82161148012). A. S. is supported by Centre for Southern Hemisphere Oceans Research (CSHOR), a joint research center between QNLM and CSIRO, and by the Australian Government's National Environmental Science Program (NESP). A.S.T. is supported by the Australian Research Council FT160100495, CE170100023, and NESP. E.E.N.M. is supported by São Paulo Research Foundation (FAPESP, Grant 20215/50122-0).

References

- Alvalá, R. C. S., Cunha, A. P. M. A., Brito, S. S. B., Seluchi, M. E., Marengo, J. A., Moraes, O. L. L., & Carvalho, M. A. (2019). Drought monitoring in the Brazilian semi-arid region. *Anais da Academia Brasileira de Ciências*, 91(suppl 1), e20170209. <https://doi.org/10.1590/0001-3765201720170209>
- Boers, N., Bookhagen, B., Marwan, N., Kurths, J., & Marengo, J. (2013). Complex networks identify spatial patterns of extreme rainfall events of the South American Monsoon system. *Geophysical Research Letters*, 40(16), 4386–4392. <https://doi.org/10.1002/grl.50681>
- Boers, N., Goswami, B., Rheinwalt, A., Bookhagen, B., Hoskins, B., & Kurths, J. (2019). Complex networks reveal global pattern of extreme-rainfall teleconnections. *Nature*, 566(7744), 373–377. <https://doi.org/10.1038/s41586-018-0872-x>
- Brito, S. S. B., Cunha, A. P. M. A., Cunningham, C. C., Alvalá, R. C., Marengo, J. A., & Carvalho, M. A. (2018). Frequency, duration and severity of drought in the semi-arid Northeast Brazil region. *International Journal of Climatology*, 38(2), 517–529. <https://doi.org/10.1002/joc.5225>
- Cai, W., McPhaden, M. J., Grimm, A. M., Rodrigues, R. R., Taschetto, A. S., Garreaud, R. D., et al. (2020). Climate impacts of the El Niño–Southern oscillation on South America. *Nature Reviews Earth & Environment*, 1(4), 215–231. <https://doi.org/10.1038/s43017-020-0040-3>
- Cai, W., Santoso, A., Collins, M., Dewitte, B., Karamperidou, C., Kug, J.-S., et al. (2021). Changing El Niño–Southern oscillation in a warming climate. *Nature Reviews Earth & Environment*, 2(9), 628–644. <https://doi.org/10.1038/s43017-021-00199-z>
- Casselmann, J. W., Taschetto, A. S., & Domeisen, D. I. V. (2021). Nonlinearity in the pathway of El Niño–Southern oscillation to the tropical North Atlantic. *Journal of Climate*, 34(17), 7277–7296. <https://doi.org/10.1175/jcli-d-20-0952.1>
- Chang, P. P., Fang, Y., Saravanan, R., Ji, L., & Seidel, H. (2006). The cause of the fragile relationship between the Pacific El Niño and the Atlantic El Niño. *Nature*, 443(7109), 324–328. <https://doi.org/10.1038/nature05053>
- Chen, M., Shi, W., Xie, P., Silva, V. B. S., Kousky, V. E., Wayne Higgins, R., & Janowiak, J. E. (2008). Assessing objective techniques for gauge-based analyses of global daily precipitation. *Journal of Geophysical Research*, 113(D4), D04110. <https://doi.org/10.1029/2007jd009132>
- Donges, J. F., Schleussner, C.-F., Siegmund, J. F., & Donner, R. V. (2016). Event coincidence analysis for quantifying statistical interrelationships between event time series. *The European Physical Journal - Special Topics*, 225(3), 471–487. <https://doi.org/10.1140/epjst/e2015-50233-y>
- Gelbrecht, M., Boers, N., & Kurths, J. (2018). Phase coherence between precipitation in South America and Rossby waves. *Science Advances*, 4(12), eaau3191. <https://doi.org/10.1126/sciadv.aau3191>
- Ham, Y.-G., Kug, J.-S., Park, J.-Y., & Jin, F.-F. (2013). Sea surface temperature in the north tropical Atlantic as a trigger for El Niño/Southern Oscillation events. *Nature Geoscience*, 6(2), 112–116. <https://doi.org/10.1038/ngeo1686>
- Hastenrath, S. (1990). Prediction of Northeast Brazil rainfall anomalies. *Journal of Climate*, 3(8), 893–904. [https://doi.org/10.1175/1520-0442\(1990\)003<0893:ponbra>2.0.co;2](https://doi.org/10.1175/1520-0442(1990)003<0893:ponbra>2.0.co;2)
- Hastenrath, S., & Heller, L. (1977). Dynamics of climatic hazards in northeast Brazil. *Quarterly Journal of the Royal Meteorological Society*, 103(435), 77–92. <https://doi.org/10.1002/qj.49710343505>
- Huang, B., Liu, C., Banzon, V., Freeman, E., Graham, G., Hankins, B., et al. (2021). Improvements of the daily optimum interpolation sea surface temperature (DOISST) version 2.1. *Journal of Climate*, 34(8), 2923–2939. <https://doi.org/10.1175/jcli-d-20-0166.1>
- Kane, R. (1997). Prediction of droughts in North–East Brazil: Role of ENSO and use of periodicities. *International Journal of Climatology*, 17(6), 655–665. [https://doi.org/10.1002/\(sici\)1097-0088\(199705\)17:6<655::aid-joc144>3.0.co;2-1](https://doi.org/10.1002/(sici)1097-0088(199705)17:6<655::aid-joc144>3.0.co;2-1)
- Kayano, M. T., & Andreoli, R. V. (2006). Relationships between rainfall anomalies over northeastern Brazil and the El Niño–southern oscillation. *Journal of Geophysical Research*, 111(D13), D13101. <https://doi.org/10.1029/2005jd006142>
- Kayano, M. T., Andreoli, R. V., Garcia, S. R., & de Souza, R. A. F. (2018). How the two nodes of the tropical Atlantic sea surface temperature dipole relate the climate of the surrounding regions during austral autumn. *International Journal of Climatology*, 38(8), 3927–3941. <https://doi.org/10.1002/joc.5545>
- Lejeune, Q., Davin, E. L., Guillod, B. P., & Seneviratne, S. I. (2015). Influence of Amazonian deforestation on the future evolution of regional surface fluxes, circulation, surface temperature and precipitation. *Climate Dynamics*, 44(9–10), 2769–2786. <https://doi.org/10.1007/s00382-014-2203-8>
- Ludescher, J., Gozolchiani, A., Bogachev, M. I., Bunde, A., Havlin, S., & Schellnhuber, H. J. (2014). Very early warning of next El Niño. *Proceedings of the National Academy of Sciences of the United States of America*, 111(6), 2064–2066. <https://doi.org/10.1073/pnas.1323058111>
- Ludescher, J., Martin, M., Boers, N., Bunde, A., Ciemer, C., Fan, J., et al. (2021). Network-based forecasting of climate phenomena. *Proceedings of the National Academy of Sciences of the United States of America*, 118(47). <https://doi.org/10.1073/pnas.1922872118>
- Malik, N., Bookhagen, B., Marwan, N., & Kurths, J. (2012). Analysis of spatial and temporal extreme monsoonal rainfall over South Asia using complex networks. *Climate Dynamics*, 39(3–4), 971–987. <https://doi.org/10.1007/s00382-011-1156-4>
- Maraun, D., & Kurths, J. (2005). Epochs of phase coherence between El Niño/Southern oscillation and Indian monsoon. *Geophysical Research Letters*, 32(15), GL023225. <https://doi.org/10.1029/2005gl023225>
- Marengo, J. A., Cunha, A. P., Soares, W. R., Torres, R. R., Alves, L. M., de Barros Brito, S. S., & Magalhaes, A. R. (2019). Increase risk of drought in the semi-arid lands of Northeast Brazil due to regional warming above 4°C. In C. A. Nobre, J. A. Marengo, & W. R. Soares (Eds.), *Climate change risks in Brazil* (pp. 181–200). Springer International Publishing.
- Marengo, J. A., Souza, C. M., Thonicke, K., Burton, C., Halladay, K., Betts, R. A., et al. (2018). Changes in climate and land use over the Amazon region: Current and future variability and trends. *Frontiers of Earth Science*, 6, 228. <https://doi.org/10.3389/feart.2018.00228>
- Marengo, J. A., Torres, R. R., & Alves, L. M. (2017). Drought in Northeast Brazil—Past, present, and future. *Theoretical and Applied Climatology*, 129(3), 1189–1200. <https://doi.org/10.1007/s00704-016-1840-8>
- McKee, T., Doesken, N., & Kleist, J. (1993). The relationship of drought frequency and duration to time scales. In *Proceedings of the 8th conference on applied climatology* (Vol. 17, pp. 179–183).
- Meng, J., Fan, J., Ludescher, J., Agarwal, A., Chen, X., Bunde, A., et al. (2020). Complexity-based approach for El Niño magnitude forecasting before the spring predictability barrier. *Proceedings of the National Academy of Sciences of the United States of America*, 117(1), 177–183. <https://doi.org/10.1073/pnas.1917007117>

- Moura, A. D., & Shukla, J. (1981). On the dynamics of droughts in Northeast Brazil: Observations, theory and numerical experiments with a general circulation model. *Journal of the Atmospheric Sciences*, 38(12), 2653–2675. [https://doi.org/10.1175/1520-0469\(1981\)038<2653:otdodi>2.0.co;2](https://doi.org/10.1175/1520-0469(1981)038<2653:otdodi>2.0.co;2)
- Quián Quiroga, R., Kreuz, T., & Grassberger, P. (2002). Event synchronization: A simple and fast method to measure synchronicity and time delay patterns. *Physical Review E - Statistical Physics, Plasmas, Fluids, and Related Interdisciplinary Topics*, 66(4), 041904. <https://doi.org/10.1103/physreve.66.041904>
- Rodrigues, R. R., Haarsma, R. J., Campos, E. J. D., & Ambrizzi, T. (2011). The impacts of inter-El Niño variability on the Tropical Atlantic and Northeast Brazil climate. *Journal of Climate*, 24(13), 3402–3422. <https://doi.org/10.1175/2011jcli3983.1>
- Rodrigues, R. R., & McPhaden, M. J. (2014). Why did the 2011–2012 La Niña cause a severe drought in the Brazilian Northeast? *Geophysical Research Letters*, 41(3), 1012–1018. <https://doi.org/10.1002/2013gl058703>
- Rosenblum, M. G., Pikovsky, A. S., & Kurths, J. (1996). Phase Synchronization of chaotic oscillators. *Physical Review Letters*, 76(11), 1804–1807. <https://doi.org/10.1103/physrevlett.76.1804>
- Singh, M., Krishnan, R., Goswami, B., Choudhury, A. D., Swapna, P., Vellore, R., et al. (2020). Fingerprint of volcanic forcing on the ENSO–Indian monsoon coupling. *Science Advances*, 6(38), eaba8164. <https://doi.org/10.1126/sciadv.aba8164>
- Taschetto, A. S., Rodrigues, R. R., Meehl, G. A., McGregor, S., & England, M. H. (2016). How sensitive are the Pacific-tropical North Atlantic teleconnections to the position and intensity of El Niño-related warming? *Climate Dynamics*, 46(5–6), 1841–1860. <https://doi.org/10.1007/s00382-015-2679-x>
- Timmermann, A., An, S.-I., Kug, J.-S., Jin, F.-F., Cai, W., Capotondi, A., et al. (2018). El Niño Southern oscillation complexity. *Nature*, 559(7715), 535–545. <https://doi.org/10.1038/s41586-018-0252-6>
- Trenberth, K. E. (1997). The definition of El Niño. *Bulletin America Meteorology Social*, 78(12), 2771–2777. [https://doi.org/10.1175/1520-0477\(1997\)078<2771:tdoen>2.0.co;2](https://doi.org/10.1175/1520-0477(1997)078<2771:tdoen>2.0.co;2)
- Uvo, C. B., Repelli, C. A., Zebiak, S. E., & Kushnir, Y. (1998). The relationships between tropical Pacific and Atlantic SST and Northeast Brazil monthly precipitation. *Journal of Climate*, 11(4), 551–562. [https://doi.org/10.1175/1520-0442\(1998\)011<0551:trbtpa>2.0.co;2](https://doi.org/10.1175/1520-0442(1998)011<0551:trbtpa>2.0.co;2)
- Wang, C. (2004). ENSO, Atlantic climate variability, and the Walker and Hadley circulations. In H. F. Diaz, & R. S. Bradley (Eds.), *The Hadley circulation: Present, past and future* (pp. 173–202). Springer Netherlands.
- Wang, L., Yu, J.-Y., & Paek, H. (2017). Enhanced biennial variability in the Pacific due to Atlantic capacitor effect. *Nature Communications*, 8(1), 14887. <https://doi.org/10.1038/ncomms14887>
- Wiedermann, M., Radebach, A., Donges, J. F., Kurths, J., & Donner, R. V. (2016). A climate network-based index to discriminate different types of El Niño and La Niña. *Geophysical Research Letters*, 43(13), 7176–7185. <https://doi.org/10.1002/2016gl069119>
- Wu, H., Svoboda, M. D., Hayes, M. J., Wilhite, D. A., & Wen, F. (2007). Appropriate application of the standardized precipitation index in arid locations and dry seasons. *International Journal of Climatology*, 27(1), 65–79. <https://doi.org/10.1002/joc.1371>
- Wu, H., Zou, Y., Alves, L. M., Macau, E. E. N., Sampaio, G., & Marengo, J. A. (2020). Uncovering episodic influence of oceans on extreme drought events in Northeast Brazil by ordinal partition network approaches. *Chaos*, 30(5), 053104. <https://doi.org/10.1063/5.0004348>
- Zou, Y., Macau, E. E. N., Sampaio, G., Ramos, A. M. T., & Kurths, J. (2018). Characterizing the exceptional 2014 drought event in São Paulo by drought period length. *Climate Dynamics*, 51(1–2), 433–442. <https://doi.org/10.1007/s00382-017-3932-2>

References From the Supporting Information

- Andreoli, R. V., de Oliveira, S. S., Kayano, M. T., Viegas, J., de Souza, R. A. F., & Candido, L. A. (2017). The influence of different El Niño types on the South American rainfall. *International Journal of Climatology*, 37(3), 1374–1390. <https://doi.org/10.1002/joc.4783>
- Palus, M., Kurths, J., Schwarz, U., Seehafer, N., Novotna, D., & Charvatova, I. (2007). The solar activity cycle is weakly synchronized with the solar inertial motion. *Physics Letters A*, 365(5), 421–428. <https://doi.org/10.1016/j.physleta.2007.01.039>
- Tedeschi, R. G., Grimm, A. M., & Cavalcanti, I. F. A. (2015). Influence of Central and East ENSO on extreme events of precipitation in South America during austral spring and summer. *International Journal of Climatology*, 35(8), 2045–2064. <https://doi.org/10.1002/joc.4106>
- Tedeschi, R. G., Grimm, A. M., & Cavalcanti, I. F. A. (2016). Influence of Central and East ENSO on precipitation and its extreme events in South America during austral autumn and winter. *International Journal of Climatology*, 36(15), 4797–4814. <https://doi.org/10.1002/joc.4670>